



Pharmacological Elevation of Circulating Bioactive Phosphosphingolipids Enhances Myocardial Recovery After Acute Infarction

YURI M. KLYACHKIN,^a PRABAKARA R. NAGAREDDY,^a SHAOJING YE,^a MARCIN WYSOCZYNSKI,^b AHMED ASFOUR,^a ERHE GAO,^c MANJULA SUNKARA,^a JA A. BRANDON,^a RAHUL ANNABATHULA,^a RAKESH PONNAPUREDDY,^b MATEESH SOLANKI,^b ZAHIDA H. PERVAIZ,^a SUSAN S. SMYTH,^a MARIUSZ Z. RATAJCZAK,^d ANDREW J. MORRIS,^a AHMED ABDEL-LATIF^a

Key Words. Sphingosine-1 phosphate • Ceramide-1 phosphate • Sphingosine-1 phosphate lyase • Tetrahydroxybutylimidazole • Mobilization • Myocardial infarction • Regeneration • Stem cells

ABSTRACT

Acute myocardial infarction (AMI) triggers mobilization of bone marrow (BM)-derived stem/progenitor cells (BMSPCs) through poorly understood processes. Recently, we postulated a major role for bioactive lipids such as sphingosine-1 phosphate (S1P) in mobilization of BMSPCs into the peripheral blood (PB). We hypothesized that elevating S1P levels after AMI could augment BMSPC mobilization and enhance cardiac recovery after AMI. After AMI, elevating bioactive lipid levels was achieved by treating mice with the S1P lyase inhibitor tetrahydroxybutylimidazole (THI) for 3 days (starting at day 4 after AMI) to differentiate between stem cell mobilization and the known effects of S1P on myocardial ischemic pre- and postconditioning. Cardiac function was assessed using echocardiography, and myocardial scar size evolution was examined using cardiac magnetic resonance imaging. PB S1P and BMSPCs peaked at 5 days after AMI and returned to baseline levels within 10 days ($p < .05$ for 5 days vs. baseline). Elevated S1P paralleled a significant increase in circulating BMSPCs ($p < .05$ vs. controls). We observed a greater than twofold increase in plasma S1P and circulating BMSPCs after THI treatment. Mechanistically, enhanced BMSPC mobilization was associated with significant increases in angiogenesis, BM cell homing, cardiomyocytes, and c-Kit cell proliferation in THI-treated mice. Mice treated with THI demonstrated better recovery of cardiac functional parameters and a reduction in scar size. Pharmacological elevation of plasma bioactive lipids after AMI could contribute to BMSPC mobilization and could represent an attractive strategy for enhancing myocardial recovery and improving BMSC targeting. *STEM CELLS TRANSLATIONAL MEDICINE* 2015;4:1333–1343

SIGNIFICANCE

Acute myocardial infarction (AMI) initiates innate immune and reparatory mechanisms through which bone marrow-derived stem/progenitor cells (BMSPCs) are mobilized toward the ischemic myocardium and contribute to myocardial regeneration. Although it is clear that the magnitude of BMSPC mobilization after AMI correlates with cardiac recovery, the molecular events driving BMSPC mobilization and homing are poorly understood. The present study confirms the role of bioactive lipids in BMSPC mobilization after AMI and proposes a new strategy that improves cardiac recovery. Inhibiting sphingosine-1 phosphate (S1P) lyase (SPL) allows for the augmentation of the plasma levels of S1P and stem cell mobilization. These findings demonstrate that early transient SPL inhibition after MI correlates with increased stem cell mobilization and their homing to the infarct border zones. Augmenting BMSPC mobilization correlated with the formation of new blood vessels and cardiomyocytes and c-Kit cell proliferation. These novel findings on the cellular level were associated with functional cardiac recovery, reduced adverse remodeling, and a decrease in scar size. Taken together, these data indicate that pharmacological elevation of bioactive lipid levels can be beneficial in the early phase after cardiac ischemic injury. These findings provide the first evidence that a carefully timed transient pharmacological upregulation of bioactive lipids after AMI could be therapeutic, because it results in significant cardiac structural and functional improvements.

^aGill Heart Institute and Division of Cardiovascular Medicine, University of Kentucky, Lexington, Kentucky, USA, and Veterans Affairs Medical Center, Lexington, Kentucky, USA;

^bInstitute of Molecular Cardiology, University of Louisville, Louisville, Kentucky, USA; ^cCenter for Translational Medicine, Temple University School of Medicine, Philadelphia, Pennsylvania, USA; ^dStem Cell Biology Institute, James Graham Brown Cancer Center, University of Louisville, Louisville, Kentucky, USA

Correspondence: Ahmed Abdel-Latif, M.D., Ph.D., Lexington Veterans Affairs Medical Center and Saha Cardiovascular Research Center, University of Kentucky, 741 South Limestone, BBSRB B349, Lexington, Kentucky 40536-0509, USA. Telephone: 859-323-6036; E-Mail: abdel-latif@uky.edu

Received November 29, 2014; accepted for publication July 8, 2015; published Online First on September 14, 2015.

©AlphaMed Press
1066-5099/2015/\$20.00/0

<http://dx.doi.org/10.5966/sctm.2014-0273>

INTRODUCTION

Acute myocardial infarction (AMI) results in ischemic heart disease (IHD), the leading cause of morbidity and mortality in the United States and Western world [1]. The prognosis of AMI and IHD remains poor despite significant advances in medical therapy and revascularization strategies [2]. Although heart transplantation remains the only option to replace the damaged myocardium, it has been limited by the availability of organ donors and postoperative complications such as graft rejection and requires continuous use of immunosuppressive drugs. The shortage of donor hearts and an ever increasing population of patients with IHD justify the need for the development of new myocardial regenerative therapies.

During the lifespan of an adult mammalian heart, up to one half of the cardiomyocytes are replenished from a poorly defined cellular source via a dynamic, but yet unclear, mechanism [3, 4]. This process is highly responsive to myocardial injury in both human subjects and rodent models, with mobilization of bone marrow (BM) resident stem cells playing a potential role in myocardial repair [5, 6]. AMI initiates a systemic inflammatory response, triggering a signaling cascade that results in egress of bone marrow stem/progenitor cells (BMSPCs) from the BM. Specifically, a continuous chemotactic gradient balance between the BM and the peripheral blood (PB) is responsible for BMSPC release. Accordingly, these mobilized PB cells, such as very small embryonic-like stem cells, *Sca1*⁺/*c-Kit*⁺/lineage-negative (*Lin*⁻) (SKL) cells, mesenchymal stem cells [7], and endothelial progenitor cells [8, 9], which are responsive to sphingosine-1 phosphate (S1P) and ceramide-1 phosphate (C1P) gradients, might home to the injured myocardium as postulated and play a role in cardiac remodeling and myocardial recovery [10].

α -Chemokine stromal-derived factor 1 (SDF-1) is considered one of the major chemotactic factors responsible for BMSPC egress and is significantly upregulated in the infarcted myocardium during the events of AMI [11]. Both SDF-1 and its receptor, CXCR4, are highly expressed by osteoblasts and fibroblasts in the BM microenvironment, and their interaction results in the retention of BMSPCs within the BM niches [12]. Although the systemic inflammatory response after AMI yields a proteolytic environment that disrupts the SDF-1-CXCR4 axis contributing to BMSPC release, it also contributes to proteolytic degradation of SDF-1 and other chemokines at the injured myocardium, suggesting alternative mechanisms for BMSPC mobilization after AMI [13, 14]. Recently, these findings have led to investigations of alternative mediators, in particular, proteolysis-resistant phosphosphingolipids, specifically S1P and C1P, which were shown to be potent chemoattractants for BMSPCs [15, 16] *in vitro* as regulators of BMSPC mobilization.

BMSPCs express S1P receptors (S1P1–5), with S1P receptors 1 and 3 involved in BMSPC mobilization in a dose-dependent manner [16]. Although SDF-1 still has a significant role in BMSPC mobilization, mounting evidence suggests other pathways might play a role in stem cell mobilization during ischemic tissue injury [15, 16]. We, and others, have shown that steady-state S1P plasma levels create a gradient favoring BMSPC egress from the BM, with this process significantly upregulated at the onset of AMI [6, 15, 16]. In addition, S1P signaling contributes to angiogenesis, cardiac development, and protection from ischemia-reperfusion (I/R) injury in the heart [17]. Specifically, the reduction of S1P synthesis and signaling has been implicated in I/R injury; however, increasing S1P signaling

through S1P2 and S1P3 might provide therapeutic benefits [18]. S1P lyase (SPL) irreversibly degrades S1P, thereby limiting the cardioprotective S1P pools and contributing to apoptosis. Recently, SPL activity was shown to be significantly upregulated in the cardiac tissue during ischemia and the pharmacological inhibition of SPL with tetrahydroxybutylimidazole (THI) mitigated those effects [19]. Also, SPL inhibition by THI supplementation was shown to be cardioprotective in a preconditioning *ex vivo* I/R model [19].

The information summarized above led us to hypothesize that pharmacological upregulation of bioactive lipids (S1P and C1P) via SPL inhibition with THI would promote mobilization of BMSPCs, followed by their homing to the ischemic myocardium, and ultimate physiological improvement of the AMI-damaged heart. Our studies show, for the first time, that pharmacological inhibition of SPL with THI significantly upregulated plasma S1P and C1P levels after AMI and correlated with significant upregulation in BMSPC mobilization. These phenomena correlated with significant improvement in left ventricular functional and remodeling parameters and a reduction in scar size. These findings provide the first evidence that early pharmacological upregulation of bioactive lipids via SPL inhibition after AMI significantly improves cardiac function, allowing the development of novel cardioprotective therapies.

MATERIALS AND METHODS

Animals

Generation of GFP BM Chimeras

All procedures were conducted under approval from the University of Kentucky Institutional Animal Care and Use Committee, in accordance with the NIH Guide for the Care and Use of Laboratory Animals (Department of Health and Human Services publication no. [NIH] 85-23, revised 1996). The mice were fed *ad libitum* with a normal chow diet (R36; Harlan Laboratories, South Easton, MA, <http://www.harlan.com>) and randomly assigned to experimental groups. Female recipient C57BL/6 mice (Jackson Laboratory, Bar Harbor, ME, <http://www.jax.org>), aged 5–6 weeks were lethally irradiated to consume the BM stem/progenitor cells. Irradiation was performed in two doses: the first dose was 700 rad, followed in 3 hours by a second dose of 500 rad. Male donor green fluorescent protein (GFP) transgenic mice (no. 006567; Jackson Laboratory) were anesthetized using 4% isoflurane and euthanized using a carbon dioxide overdose followed by cervical dislocation. BM was harvested from the hip bones, tibias, and femurs. The irradiated mice were injected via the lateral tail vein with 5×10^6 fresh GFP bone marrow cells in 0.3 ml of medium. Chimerism was confirmed using flow cytometric analysis of peripheral blood cells for GFP-positive cells at 6 weeks after transplantation.

Murine Model of Myocardial Infarction

The mice were anesthetized with 2% isoflurane using an inhaled delivery system. The heart was exposed and pushed out of the thorax with direct visual control, and the left anterior descending coronary artery (LAD) was sutured and ligated at a site approximately 3 mm from its origin using a 6-0 silk suture, as previously described [20]. The heart was immediately placed back into the intrathoracic space after the knot was tied, followed by manual evacuation of the pneumothorax and closure of muscle and the skin using the previously placed purse-string suture. The sham group underwent the same surgical procedure, except that the ligature was passed under the LAD but not tied.

Drug Treatment

To inhibit SPL, 4 days after surgery, the mice received vehicle or 25 mg/L THI (catalog no. T6330; Sigma-Aldrich, St. Louis, MO, <http://www.sigmaaldrich.com>) administered ad libitum in water containing 5% dextrose (to improve palatability). THI is a Food and Drug Administration-approved caramel food coloring additive, shown to inhibit SPL when administered orally to mice [19, 21]. THI treatment was administered for 3 days and stopped at day 7 after AMI. Water intake was not different between the vehicle- and THI-treated groups. The mice were injected daily with bromodeoxyuridine (BrdU) (B9285; Sigma-Aldrich) at 80 mg/kg, i.p., beginning the day of operation until sacrifice. The mice were sacrificed at 35 days after the operation via CO₂ asphyxiation, followed by cervical dislocation.

PB Collection

To assess the bioactive lipid levels, stem cell mobilization, and gene expression, PB samples were collected into tubes containing a 1:5 ratio of EDTA/citrate-theophylline-adenosine-dipyridamole (CTAD) at the indicated time points.

Histology

After final echocardiography and peripheral blood collection, the hearts were harvested in diastole with saturated KCl and CdCl (100 mM) injected through the apex into the left ventricular (LV) cavity. The LV apex was then cannulated and the heart perfused with PBS, followed by 10% buffered formalin at 75 mmHg, with the severed inferior vena cava serving as the outlet. The hearts were then cut into 2-mm cross-sectional slices and processed for paraffin embedding. The slices were cut into 4- μ m sections for histologic examination and immunofluorescent staining. The LV area, area at risk, LV cavity area, and infarct area were measured in Masson's trichrome-stained sections, as previously described [22]. Images were acquired digitally and the areas measured using NIH ImageJ, version 1.37 (NIH, Bethesda, MD, <http://www.imagej.nih.gov/ij/>). Cell turnover was evaluated by staining against BrdU (Roche, Indianapolis, IN, <http://www.roche.com>) and α -sarcomeric actin (Sigma-Aldrich) and counting BrdU⁺ cells in the infarct border regions. Regeneration was evaluated by counterstaining with BrdU and α -sarcomeric actin (Sigma-Aldrich) or myosin heavy chain (MHC) (Abcam, Cambridge, MA, <http://www.abcam.com>) and counting BrdU⁺ α -SA⁺ or BrdU⁺MHC⁺ cells in both ischemic and remote regions. c-Kit cells were quantified after staining using goat anti-mouse c-Kit polyclonal primary antibody (Sigma-Aldrich). GFP bone marrow cell mobilization and homing were measured by anti-GFP staining in infarct border regions (Abcam). The capillary density was measured in FITC-isolectin B4 (catalog no. FL1201; Vector Laboratories, Burlingame, CA, <http://www.vectorlabs.com>) stained sections.

Echocardiography

Echocardiograms were obtained using a Vevo 2100 system (VisualSonics, Toronto, CA, <http://www.visualsonics.com>) equipped with a 15-7-MHz linear broadband transducer and a 12-5-MHz phased array transducer. In vivo cardiac function was assessed at baseline before cardiac surgery, at 48 hours after MI, and immediately before sacrifice at 35 days after MI by echocardiography. Using a rectal temperature probe, body temperature was maintained carefully at 37°C throughout the study using a heating pad. Modified parasternal long-axis and

short-axis views were obtained to assess the left ventricular function and volume in M-mode, two-dimensional, and Doppler echocardiography modes. Systolic and diastolic parameters were obtained using M-Mode tracings at the mid-papillary level. The LV volumes were estimated using the Teichholz formula at end-systole and end-diastole. Echocardiography was performed with the mice under 1%–3% isoflurane anesthesia. All echocardiography analyses were performed by an investigator unaware of the groups.

Cardiac Magnetic Resonance Imaging

Cardiac magnetic resonance imaging (CMR) was performed on a 7-Tesla ClinScan system (Bruker, Ettlingen, Germany, <http://www.bruker.com>) equipped with a 4-element phased-array cardiac coil and a gradient system with a maximum strength of 450 mT/m and a maximum slew rate of 4,500 mT/m/s. We acquired whole short-axis stack images from base to apex for comparison with late enhancement images. The short-axis images were planned perpendicular to the four-chamber long-axis image. For late gadolinium-enhanced magnetic resonance imaging, a 0.6 mmol/kg bolus of gadolinium-diethylene triamine pentaacetic acid (Gd-DTPA; Magnevist, Schering Health Care, West Sussex, U.K., <http://www.schering.co.uk>) was injected using the intraperitoneal route. Imaging was initiated 10 minutes after the injection of Gd-DTPA using an electrocardiographically gated segmented magnetization-prepared fast low-angle shot sequence with a fixed inversion time at 500 ms. The CMR data were analyzed using commercially available postprocessing software: CMR42 (Circle Cardiovascular Imaging, Calgary, Alberta, Canada, <http://www.circlecvi.com>) by a single experienced reader who was unaware of the experimental data. Enhanced regions were determined by thresholding signal intensity at 5 SD above the mean signal intensity of remote normal myocardium in the same slice. A small region of interest was manually drawn and placed in remote normal myocardium (defined as normal function without enhancement on visual assessment). If a slice contained no remote normal myocardium, the mean and SD of the nearest slice with normal remote myocardium was used.

Quantitation of C1P and S1P

PB samples were obtained from the retro-orbital plexus of the mice into tubes containing a 1:5 ratio of EDTA/CTAD. Plasma was isolated by centrifuging whole blood for 10 minutes at 800g. Supernatant was then removed and centrifuged at 9,400g for 10 minutes to remove platelets, and the supernatant was then used for lipid measurements. Lipids were extracted from plasma, supernatant using acidified organic solvents, as previously described [23, 24]. An analysis of S1P and C1P was performed using a Shimadzu UFLC (Shimadzu Corp., Kyoto, Japan, <http://www.shimadzu.com>) coupled with an AB Sciex 4000-Qtrap hybrid linear ion trap triple quadrupole mass spectrometer (AB Sciex, Framingham, MA, <http://www.sciex.com>) in multiple reaction monitoring mode, as previously described [24]. The mobile phase consisted of 75/25 of methanol/water with formic acid (0.5%) and 5 mM ammonium formate (0.1%) as solvent A and 99/1 of methanol/water with formic acid (0.5%) and 5 mM ammonium formate (0.1%) as solvent B. For the analysis of various C1P species, the separation was achieved by maintaining 75% of solvent B for 3 minutes, increasing to 100% B over the next 3 minutes, and maintaining at 100% of solvent B for the last 18 minutes. The column was equilibrated back

to the initial conditions in 3 minutes. The flow rate was 0.5 ml/min with a column temperature of 60°C. The sample injection volume was 10 μ l. The mass spectrometer was operated in the positive electrospray ionization mode with optimal ion source settings determined by synthetic standards with a declustering potential of 46 V, entrance potential of 10 V, collision energy of 19 V, collision cell exit potential of 14 V, curtain gas of 30 psi, ion spray voltage of 5,500 V, ion source gas 1/gas 2 of 40 psi, and temperature of 550°C.

Flow Cytometry

SKL (Sca1⁺c-Kit⁺Lin⁻) staining was performed in 50 μ l of PB after removing the plasma collected from the retro-orbital plexus of the mice into tubes containing a 1:5 ratio of EDTA/CTAD. PB was resuspended in PBS containing 2% fetal bovine serum. First, the stem cell monoclonal antibodies (mAbs) were added at saturating concentrations, and the cells were incubated for 20 minutes on ice, followed by 30 minutes of ice incubation with mAbs against the lineage markers. The cells were lysed, fixed with 1 \times lyse/fix buffer (catalog no. 558049; BD Pharmingen, San Diego, CA, <http://www.bdbiosciences.com>) and analyzed by LSR II (Becton Dickinson and Co., Mountain View, CA, <http://www.bd.com>). Stem cells were detected with anti-mouse Abs against CD45 PE (catalog no. 553081; BD Pharmingen, San Jose, CA, <http://www.bdbiosciences.com>), CD90.2 PerCP (catalog no. 140316; BioLegend, San Diego, CA, <http://www.biolegend.com>), and aLy-6A/E PECy7 (Sca-1) (catalog no. 558162; BD Pharmingen). All anti-mouse lineage markers (Lin) were FITC conjugated and purchased from BD Pharmingen: anti-CD45R/B220 (catalog no. 553088); anti-T-cell receptor- β (TCR- β ; catalog no. 553170); anti-TCR- $\gamma\delta$ (catalog no. 553177); anti-CD11b (catalog no. 553310); anti-Ter-119 (catalog no. 557915); and anti-Ly6G and Ly6C (catalog no. 553127).

Real-Time Polymerase Chain Reaction

Total mRNA was isolated from the PB with the RNeasy Mini Kit (Qiagen Inc., Valencia, CA, <http://www.qiagen.com>) and reverse-transcribed with TaqMan Reverse Transcription Reagents (Applied Biosystems, Foster City, CA, <http://www.appliedbiosystems.com>). Quantitative assessment of mRNA expression of markers characterizing endothelial cell (vascular endothelial growth factor [VEGF]), cardiac cells (vascular endothelial [VE]-cadherin), homing factors (SDF-1 and CXCR4), and β_2 -microglobulin was performed by quantitative reverse transcription-polymerase chain reaction (RT-PCR) using a StepOnePlus real-time thermocycler (Applied Biosystems). Relative quantitation of mRNA expression was performed with the comparative Ct method. The relative quantitative value of target, normalized to an endogenous control (β_2 -microglobulin gene) and relative to a calibrator, was expressed as $2^{-\Delta\Delta Ct}$ (x -fold difference), where $\Delta Ct = (Ct \text{ of target genes } [Oct-4, Nanog, Rex-1, Rif1, Dppa1, Gata4, Nkx2.5]) - (Ct \text{ of endogenous control gene } [\beta_2\text{-microglobulin}])$, and $\Delta\Delta Ct = (\Delta Ct \text{ of samples for target gene}) - (\Delta Ct \text{ of calibrator for the target gene})$. To avoid the possibility of amplifying contaminating DNA (a) all primers for real-time RT-PCR were designed to span an intron for specific cDNA amplification; (b) reactions were performed with appropriate negative controls (template-free controls); (c) a uniform amplification of the products was rechecked by analyzing the melting curves of the amplified products (dissociation graphs); and (d) the melting temperature

(Tm) was 57°C–60°C, and the probe Tm was at least 10°C higher than the primer Tm. Three independent experiments were performed for each set of genes.

Statistical Analysis

Data are expressed as mean \pm SEM. Differences were analyzed using the unpaired Student t test or analysis of variance (one-way or multiple comparisons), as appropriate. Post hoc multiple comparison procedures were performed using two-sided Dunnett or Dunn tests, as appropriate, with control samples as the control category. A value of $p < .05$ was considered significant. All statistical analyses were performed using the Prism, version 6, package (GraphPad, La Jolla, CA, <http://www.graphpad.com>). All of us had full access to, and took full responsibility for, the integrity of the data and have read and agreed with the report as written.

RESULTS

SPL Inhibition Elevates S1P Levels After MI and Contributes to Stem Cell Mobilization

The optimal timing of stem cell arrival, survival, proliferation, and self-renewal at the sites of myocardial infarction is largely determined by the conditions of the myocardial microenvironment. The induction of MI generates a robust proinflammatory state with the generation of reactive oxygen species and a cytokine cascade, which contributes to neutrophil infiltration, peaking between 24 and 72 hours after MI [25]. This, combined with reduced perfusion of the infarct region, contributes to a myocardial microenvironment that is unsuitable for stem cell survival. However, approximately 5 days after MI, the local acute inflammation subsides, and the initiation of angiogenesis creates a desirable, yet transient, environment for stem cells to home and proliferate [26]. This window of opportunity for stem cell homing is limited by subsequent fibrosis and scar formation at the infarct site by 10–14 days after MI, which hinders stem cell nesting and the potential benefit [26]. To determine whether elevating S1P levels will enhance stem cell mobilization [6, 15, 16], we inhibited SPL at days 4–7 after MI to optimize the timing for stem cell mobilization to the injured myocardium. THI, an S1P lyase inhibitor, was administered in drinking water on days 4–7 after MI. We used a previously described dosing of 25 mg/l, because it yielded maximal changes in plasma bioactive lipids during in vivo experiments [19]. Initially, a proof of concept experiment was performed to assess THI efficacy in elevating plasma bioactive lipids and stem cell mobilization. THI administration for 3 days under physiological conditions significantly elevated total plasma S1P (0.3 ± 0.04 vs. 0.76 ± 0.03 μ M; $p < .05$) and C1P (0.24 ± 0.01 vs. 1.3 ± 0.2 μ M; $p < .05$) levels in control mice (Fig. 1A, 1B), suggesting robust SPL inhibition. THI administration also contributed to significant elevation in circulating stem cells such as Sca1⁺, c-Kit⁺, lineage-negative (SKL) cells (33 ± 5 vs. 237 ± 33 cells per 50 μ l of PB; $p < .05$) and Lin⁻/CD45⁻/Sca1⁺ cells (45 ± 8 vs. 359 ± 27 cells per 50 μ l of PB; $p < .05$; Fig. 1C, 1D), suggesting that SPL inhibition and subsequent elevation in plasma bioactive lipid levels contributes to stem cell mobilization. THI therapy has no effect on cardiac function in healthy mice under physiological conditions. Although the effects of AMI alone resulted in significant elevation of plasma bioactive lipid levels and circulating stem cells,

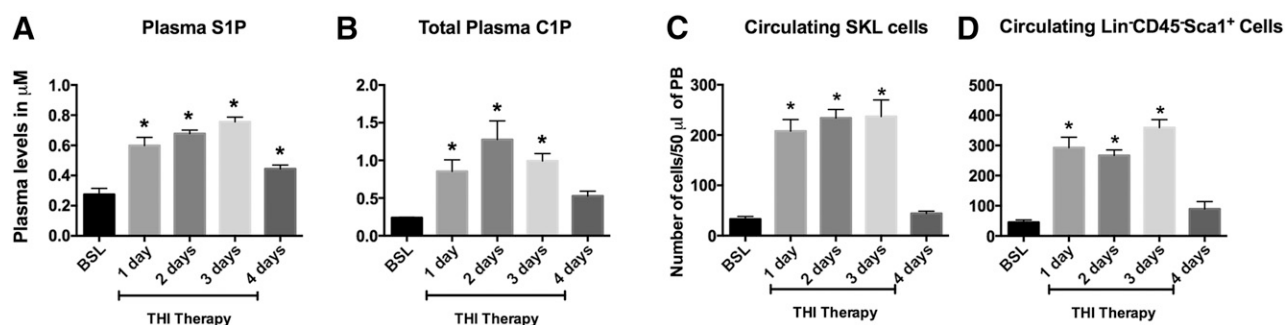


Figure 1. THI treatment increased bioactive lipid levels and stem cell mobilization in the peripheral blood after THI treatment ($n = 4$ per time point per group of mice). Bar graphs show significant upregulation of plasma S1P and C1P during 3 days of THI supplementation in healthy mice (**A, B**). THI supplementation also contributes to significant upregulation in stem cell mobilization (**C, D**). Values are presented as mean \pm SEM (*, $p < .05$ compared with baseline values). Abbreviations: BSL, baseline; C1P, ceramide-1 phosphate; S1P, sphingosine-1 phosphate; SKL, Sca1⁺c-Kit⁺Lin⁻ (lineage-negative) murine stem cells; THI, tetrahydroxybutylimidazole.

THI administration improved these effects by increasing S1P and C1P levels and prolonging these effects to beyond day 7 after MI (S1P, 0.45 ± 0.06 vs. 0.70 ± 0.05 μM at day 5 and 0.47 ± 0.03 vs. 0.80 ± 0.02 μM at day 7, $p < .05$; C1P, 1.1 ± 0.1 vs. 1.4 ± 0.2 μM at day 5 and 0.62 ± 0.1 vs. 1.5 ± 0.2 μM at day 7, $p < .05$; Fig. 2A, 2B). Mobilization of multiple stem cell populations was similarly augmented at day 5 and prolonged beyond day 7 after MI with THI treatment (SKL cells, 249 ± 34 vs. 347 ± 53 cells per $50 \mu\text{l}$ of PB at day 5 and 54 ± 11 vs. 155 ± 25 cells per $50 \mu\text{l}$ of PB at day 7; Lin⁻/CD45⁻/Sca1⁺, 176 ± 14 vs. 327 ± 19 cells per $50 \mu\text{l}$ of PB at day 5 and 90 ± 2 vs. 228 ± 10 cells per $50 \mu\text{l}$ of PB at day 7; Lin⁻/CD45⁻/Thy1.1⁺, 232 ± 24 vs. 387 ± 40 cells per $50 \mu\text{l}$ of PB at day 5 and 237 ± 22 vs. 398 ± 79 cells per $50 \mu\text{l}$ of PB at day 7; $p < .05$ for all comparisons; Fig. 2C, 2D; supplemental online Fig. 1). It is important to note that SPL inhibition had no significant difference on the white blood cell counts between the THI-treated and nontreated cohorts (supplemental online Fig. 2).

SPL Inhibition Increases Circulating BMSPCs, Which Express Genes Responsible for Angiogenesis and Cell Survival After MI

Stem and progenitor cells mobilized after MI are enriched in subpopulations that express angiogenic and promobilization factors considered important for tissue regeneration [27, 29]. To assess whether THI-mobilized BMSPCs are also enriched in angiogenic factors, we measured the mRNA expression levels of endothelial genes such as VEGF and VE-cadherin and factors involved in stem cell mobilization and homing such as SDF-1 and CXCR4 at various time points after MI by quantitative RT-PCR. THI administration was associated with higher expression of proangiogenic endothelial genes, VEGF (2.4 ± 0.8 vs. 3.1 ± 0.6 fold change at day 5 and 0.3 ± 0.1 vs. 1.2 ± 0.3 fold change at day 7, $p < .05$ for all comparisons) and VE-cadherin (2.8 ± 0.9 vs. 4.3 ± 1.1 fold change at day 5 and 1.2 ± 0.2 vs. 5.3 ± 1 fold change at day 7, $p < .05$ for all comparisons; Fig. 3A, 3B), and of SDF-1 (1.5 ± 0.3 vs. 7.4 ± 1 fold change at day 5 and 7 ± 2 vs. 32 ± 4 fold change at day 7, $p < .05$ for all comparisons) and CXCR4 (3.5 ± 0.5 vs. 8.1 ± 1.6 fold change at day 7, $p < .05$; Fig. 3C, 3D). Our published data and data from other laboratories have demonstrated that S1P can initiate angiogenesis and upregulation of BM-derived endothelial cells [29, 30]. However, we cannot exclude other pathways initiated by myocardial injury to be responsible for the increased expression of endothelial genes and angiogenesis

in our model. Nonetheless, THI treatment augmented this existing phenomenon and could be a viable therapeutic target in future studies.

SPL Inhibition Improves Myocardial Function After Coronary Artery Ligation

The clinical significance of BMSPC mobilization stems from the available evidence suggesting strong correlation between the degree of bone marrow stem cell mobilization in patients after MI and recovery of LV function [10]. We hypothesized that increased stem cell mobilization could potentially contribute to alleviating injury by augmenting regeneration. The corroborated window of time in which the long-term effects of MI in mice are observed (fibrosis, cardiac remodeling, and changes in function) has been established at 4–5 weeks after the onset of MI [31]. Therefore, we assessed the long-term effects of post-MI THI supplementation on heart function in an in vivo murine MI model at 48 hours and 5 weeks after MI via echocardiography. Both groups (vehicle- and THI-treated mice) had a similar significant reduction in cardiac functional parameters at 48 hours after MI (Fig. 4). SPL inhibition resulted in significant recovery of cardiac function at 5 weeks after MI. Specifically, SPL inhibition contributed to significant improvement in LV systolic function as seen in the elevation of the ejection fraction ($23\% \pm 2\%$ vs. $35\% \pm 3\%$; $p < .05$; Fig. 4A). Furthermore, SPL inhibition resulted in favorable remodeling of the left ventricle as evidenced by reduced left ventricular end-systolic (4.6 ± 0.2 vs. 3.6 ± 0.2 mm, $p < .05$) and end-diastolic (5.1 ± 0.2 vs. 4.3 ± 0.2 mm, $p < .05$; Fig. 4B) diameters and a reduction in LV volume at end-systole (68 ± 9 vs. 37 ± 9 μl ; $p < .05$) and end-diastole (89 ± 8 vs. 53 ± 9 μl ; $p < .05$; Fig. 4C, 4D). Enhanced stem cell mobilization was also associated with a significant increase in the infarct wall (0.5 ± 0.02 vs. 0.7 ± 0.03 mm; $p < .05$) and posterior wall thickness (0.8 ± 0.02 vs. 0.9 ± 0.03 mm; $p < .05$; Fig. 4E, 4F). Together, these results demonstrate that SPL inhibition after AMI correlates with left ventricular recovery.

SPL Inhibition Decreases Scar Size at 5 Weeks After AMI

The effect of THI supplementation on LV dilation, remodeling, and failure at 5 weeks after AMI was further characterized in Masson's trichrome-stained sections (Fig. 5A). Morphometric analysis at sacrifice, 5 weeks after AMI, demonstrated THI supplementation decreased the myocardial scar size (0.35 ± 5 vs. 0.22 ± 3 ; $p < .05$;

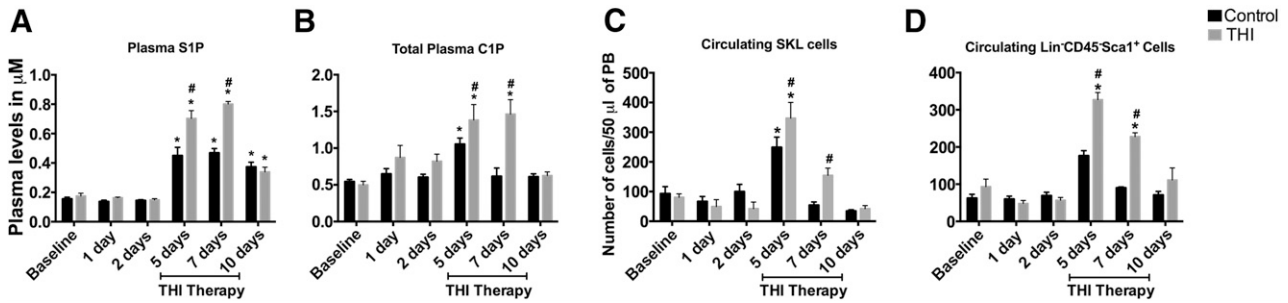


Figure 2. THI treatment augmented the upregulation of bioactive lipid levels and stem cell mobilization in the peripheral blood after myocardial infarction ($n = 7$ per time point per group). Bar graphs show significant upregulation of plasma S1P and C1P with acute myocardial infarction (A, B). Acute myocardial infarction was also associated with significant upregulation in stem cell mobilization (C, D). THI treatment augmented the endogenous response of elevated bioactive lipids and stem cell mobilization after acute myocardial infarction. Values are presented as mean \pm SEM (*, $p < .05$ compared with baseline values; #, $p < .05$ compared with vehicle controls and baseline values). Abbreviations: C1P, ceramide-1 phosphate; PB, peripheral blood; S1P, sphingosine-1 phosphate; SKL, Sca1⁺c-Kit⁺Lin⁻ (lineage-negative) murine stem cells; THI, tetrahydroxybutylimidazole.

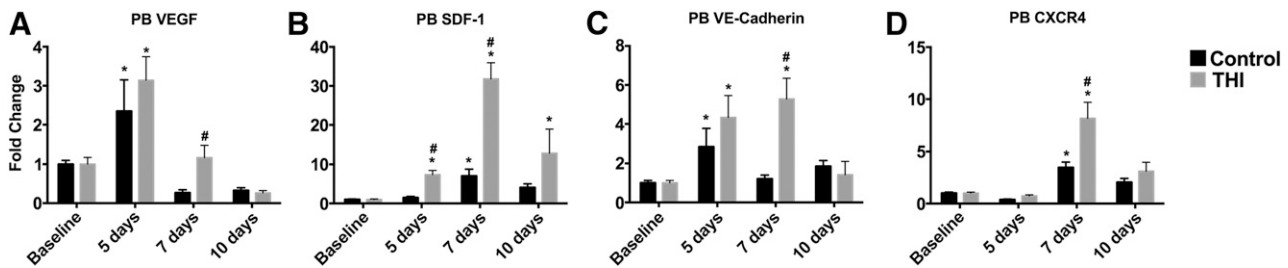


Figure 3. Sphingosine-1 phosphate lyase inhibition elevated the genes involved in stem cell survival and myocardial homing ($n = 4$ per time point per group). Bar graphs show significant upregulation of endothelial transcription factors VEGF and VE-cadherin and factors involved in stem cell homing such as SDF-1 and CXCR4 in peripheral blood cells at various time points after MI in vehicle-treated ($n = 5$) and THI-treated ($n = 5$) mice. Values are presented as mean \pm SEM (*, $p < .05$ compared with baseline values; #, $p < .05$ compared with vehicle controls and baseline values). Abbreviations: MI, myocardial infarction; PB, peripheral blood; SDF-1, stromal-derived factor 1; VE, vascular endothelial; VEGF, vascular endothelial growth factor.

Fig. 5B). We used cardiac magnetic resonance imaging, which enabled us to examine the progression of scar size between the first week and 5 weeks after AMI. The observed reduction in scar size by histologic examination was paralleled by CMR assessment. No difference was found in delayed enhancement at 5 days after AMI between the THI- and placebo-treated mice. However, at 5 weeks, the THI-treated mice showed a significantly smaller scar size as determined by the area of delayed enhancement compared with placebo-treated mice (0.33 ± 0.01 vs. 0.20 ± 0.04 ; $p < .05$; Fig. 5C, 5D). This could represent a reduction in the progression of heart failure and a slowing of scar progression by mobilized BM cells.

Increased Myocardial Homing of GFP⁺ BM Cells and Augmented Cardiomyocyte Turnover in THI-Treated Mice

To determine whether pharmacological upregulation of bioactive lipids resulted in increased stem cell homing to the infarcted myocardium, we used GFP bone marrow chimeras in our murine AMI model. At 6 weeks after transplantation, the GFP BM chimerism was confirmed via flow cytometry of the peripheral blood, which demonstrated a chimerism rate of greater than 80% ($85.3\% \pm 1\%$). We examined the homing and retention of bone marrow-derived cells by quantitating GFP⁺ cells in the peri-infarct border zone in THI-treated and vehicle control-treated mice by immunofluorescent confocal microscopy at 5 weeks after MI. THI-treated mice had more than twice the number of GFP⁺ cells in the infarct border zone than the controls 5 weeks after MI at the infarct border. However, we did not encounter significant differences at the remote zone (infarct border, 11.3 ± 1 vs. 4.1 ± 0.8

cells per 1,000 nuclei, $p < .001$; remote zone, 2.6 ± 0.3 vs. 2.8 ± 0.5 cells per 1,000 nuclei, $p = \text{NS}$; Fig. 6A, 6B). We did not see significant numbers of cardiomyocytes originating from GFP⁺ cells in either group. Similarly, we observed significantly higher numbers of BrdU⁺ cells (infarct border, 14.8 ± 1 vs. 6.1 ± 0.6 cells per 1,000 nuclei, $p < .001$; remote zone, 4.0 ± 0.6 vs. 4.4 ± 0.7 cells per 1,000 nuclei, $p = \text{NS}$; Fig. 6A, 6C) and BrdU⁺/α sarcomeric actin-positive cells (infarct border, 6.6 ± 0.5 vs. 2.3 ± 0.3 cells per 1,000 nuclei, $p < .05$; remote zone, 1.6 ± 0.2 vs. 2.3 ± 0.4 cells per 1,000 nuclei, $p = \text{NS}$; Fig. 6A, 6D) in THI-treated mice. Also, THI treatment was associated with higher rates of BrdU⁺/myosin heavy chain-positive cells at the infarct border (supplemental online Fig. 3). However, the percentage of cardiomyocyte turnover was lower with myosin heavy chain staining than with α-sarcomeric actin staining, probably reflecting its higher specificity for cardiac cells. These results show, for the first time, that pharmacological upregulation of bioactive lipids contributes to both BM mobilization and homing/retention to the infarcted myocardium.

In addition to cardiomyocyte turnover, we assessed the population of c-Kit-positive cells in the myocardium after injury. THI-treated mice had a higher number of c-Kit⁺ cells in the infarct border zone than the controls 5 weeks after MI. However, we did not observe significant differences at the remote zone (infarct border, 0.22 ± 0.03 vs. 0.3 ± 0.03 cells per nuclei, $p = .08$; remote zone, 0.22 ± 0.03 vs. 0.26 ± 0.03 cells per nuclei, $p = \text{NS}$; Fig. 6A, 6E). The rate of c-Kit cells originating from GFP BM cells in both groups was very low in both the infarct border and the remote zones ($<1\%$).

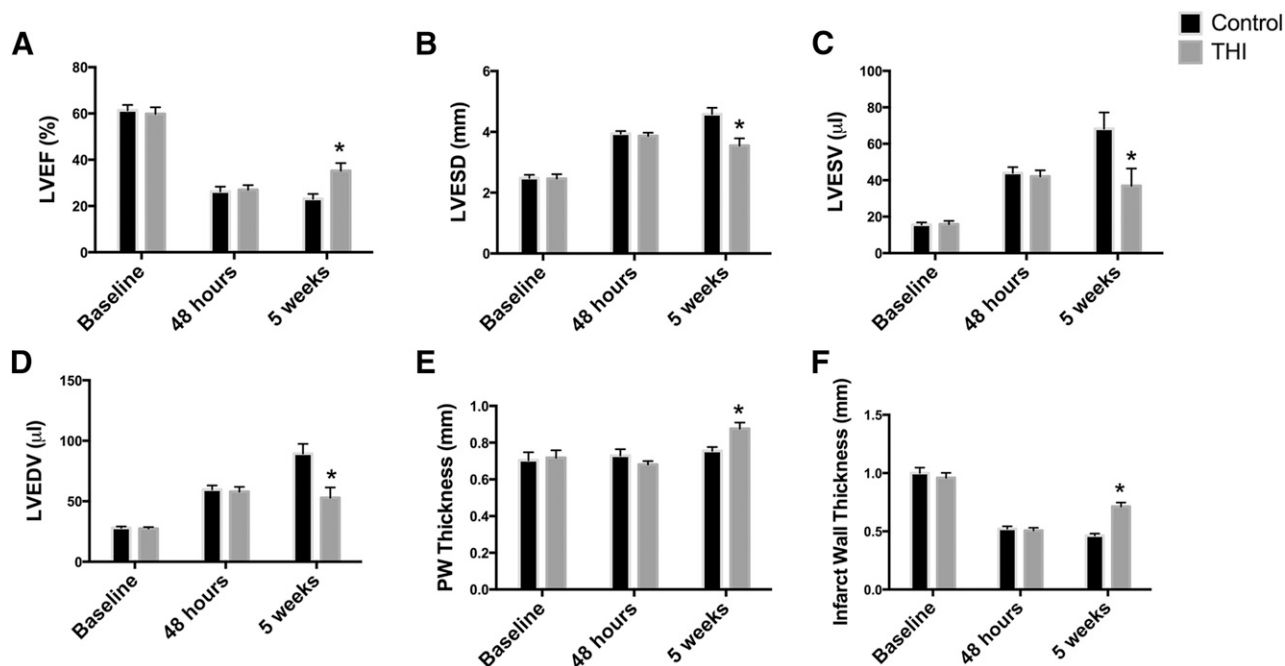


Figure 4. THI supplementation enhanced functional recovery after myocardial infarction. Echocardiographic analysis of left ventricular function and remodeling parameters. Treatment with THI enhanced cardiac recovery after acute myocardial infarction induced by left coronary artery ligation. Left ventricular ejection fraction (A), left ventricular end-systolic diameter (B) and volume (C), left ventricular end-diastolic volume (D), posterior wall (E), and infarct wall thickness (F) were assessed before infarction (baseline) and 48 hours and 5 weeks after myocardial infarction in vehicle-control ($n = 12$) and THI-treated ($n = 10$) mice. Values are presented as mean \pm SEM (*, $p < .05$ compared with controls). Abbreviations: LVEDV, left ventricular end-diastolic volume; LVEF, left ventricular ejection fraction; LVESD, left ventricular end-systolic diameter; THI, tetrahydroxybutylimidazole.

Increased Capillary Density in the Infarct Border in THI-Treated Mice

To examine the mechanisms by which SPL inhibition could improve the response to injury leading to recovery, the capillary density was assessed as an index of the heart's capacity to respond to increased stress [22]. The myocardial capillary density in at-risk and remote regions was measured in sections stained with the endothelial-specific FITC-isolectin B4. The capillary density in mice supplemented with THI was significantly increased in both the at-risk and the remote areas (infarct border, 319 ± 27 vs. 917 ± 54 , $p < .05$; remote zone, $1,300 \pm 118$ vs. $1,806 \pm 116$, $p < .05$; Fig. 7). These findings correlate with the above data, showing enhanced mobilization of stem cells enriched in endothelial progenitor cells and augmentation of endothelial gene expression in the PB after MI and with THI treatment. The observed increase in capillary density could explain the improvement noted in cardiac function and enhanced regeneration. These data are consistent with a model in which pharmacological upregulation of bioactive lipids via SPL inhibition, which contributes to an improved regenerative response after MI, improved LV function and LV remodeling.

DISCUSSION

Our findings provide evidence that pharmacological upregulation of bioactive phosphosphingolipids after AMI contributes to stem cell mobilization and homing to the infarcted myocardium, which correlated with physiological and functional improvement of the infarcted heart. Increased stem cell homing might have contributed to enhanced angiogenesis, leading to accelerated regeneration with a resulting decreased infarct scar size and significant recovery in

LV function and reduced adverse remodeling. Enhanced stem cell mobilization also correlated with increased proliferation of cardiomyocytes and c-Kit cells at the infarction border. This observation corroborates with our previous data that S1P and C1P are involved in the trafficking of BMSPCs [16, 32–35]. Importantly, our results also suggest that a carefully timed transient pharmacological upregulation of bioactive lipids after AMI can be therapeutic and will result in significant cardiac recovery after ischemic injury.

Multipotent stem cell populations are mobilized from the bone marrow into peripheral blood in response to AMI in both murine models and patients, as demonstrated by us, and others [15, 27, 36]. We have recently shown that elevation of bioactive lipids after AMI contributes to stem cell mobilization via mechanisms involving S1P/S1PR1-SDF1/CXCR4 cross-talk [15, 37]. These observations are supported in the present study by the significant upregulation of SDF-1 and CXCR4 mRNA expression in PB cells, in conjunction with elevated plasma S1P and C1P levels. Small human studies have correlated the degree of bone marrow stem cell mobilization after AMI with LV functional recovery in patients, albeit with small benefit [10]. Animal studies have demonstrated improved cardiac recovery after MI with the use of granulocyte colony-stimulating factor (G-CSF) [38]. However, the mechanisms of G-CSF-mediated regeneration and the utility of its use are still controversial. However, G-CSF therapy has yielded inconsistent results in human studies, with some studies in AMI patients showing small benefit and other studies and meta-analyses reporting largely negative results for any discernable benefit [39–41]. In the present study, we adopted a more specific and novel approach to stem cell mobilization and have shown, for the first time, the ability to upregulate BM stem cell mobilization

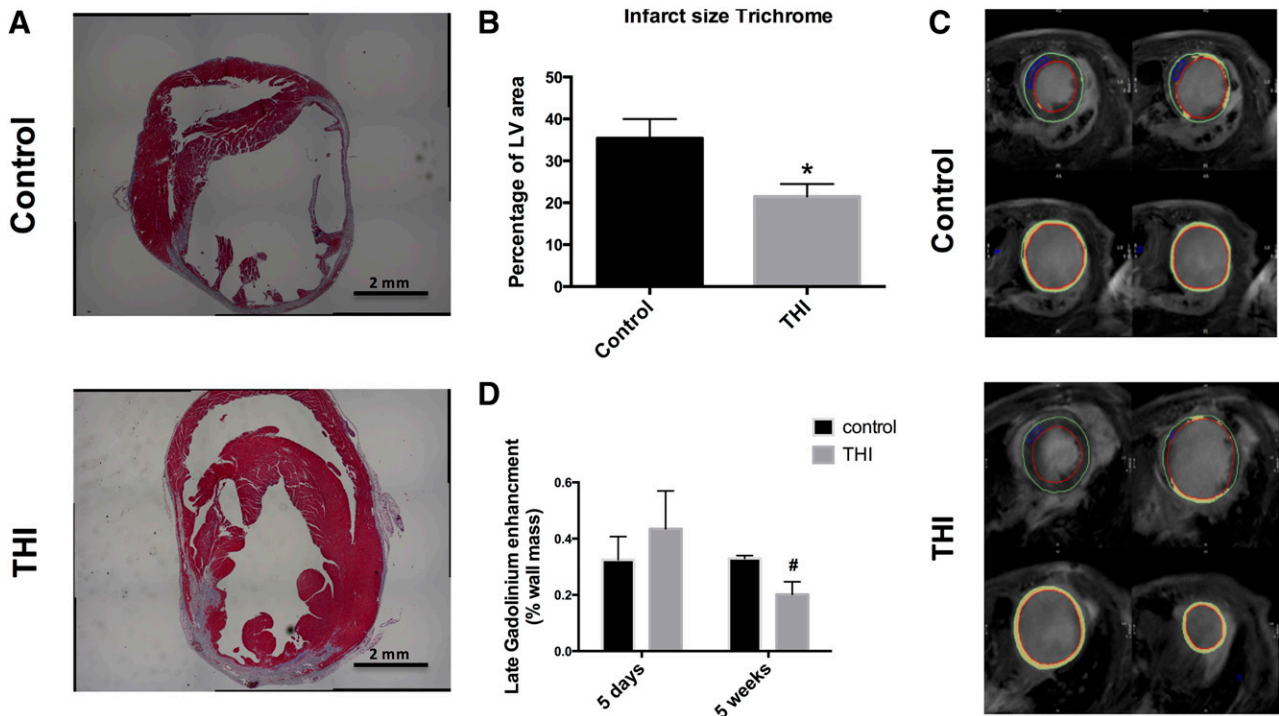


Figure 5. Morphometric analysis and cardiac magnetic resonance (CMR) assessment of left ventricular scar development. THI supplementation decreased myocardial injury and alleviated LV hypertrophy after myocardial infarction (MI). Scar and viable myocardium in the risk region were determined in Masson's trichrome-stained LV sections 35 days after myocardial infarction surgery. **(A):** Representative Masson's trichrome-stained heart short-axis sections in vehicle- and THI-treated mice. **(B):** Scar, graphed as percentage of LV area, was decreased in hearts of THI-supplemented mice after infarction. Values are presented as mean \pm SEM (vehicle-control, $n = 14$] vs. THI-treated, $n = 25$] groups). THI supplementation reduced scar progression at 5 weeks of follow-up. Scar and viable myocardium in the scar region were examined by cardiac magnetic resonance imaging using delayed enhancement at 5 days and 5 weeks after acute MI. **(C):** Representative short-axis images of CMR from vehicle-treated and THI-treated mice at 5 weeks after acute MI showing reduced scar size in the THI-treated arm. **(D):** Quantitative analysis of the scar size presented as the percentage of gadolinium enhancement of the left ventricular wall showing a similar infarct size at 5 days. At 5 weeks of follow-up, the scar size remained similar in the control-treated arm but was reduced significantly in the THI-treated arm. Values are presented as mean \pm SEM (*, $p < .05$ compared with control; and #, $p < .05$ vs. 5-day values). Vehicle treated ($n = 7$) vs. THI treated ($n = 7$). Abbreviations: LV, left ventricular; THI, tetrahydroxybutylimidazole.

after MI via SPL inhibition. Our data suggest that PB has increased gene expression of endothelial genes, and we hypothesize that this could have contributed to the increased capillary density and cardiomyocyte renewal seen after AMI and the enhanced recovery in THI-treated mice.

Cardiac recovery measured 5 weeks after MI in THI-treated mice was improved, as evidenced by the recovering LV function and reduction of LV diameter and adverse remodeling. The opposite was seen in the control-treated mice, implying progression to heart failure. Bone marrow stem cells facilitated regeneration of the heart after MI in animal models and in several clinical studies [42]. In human studies, the benefit was observed mostly in patients with reduced left ventricular function at baseline. The mechanisms through which mobilized BM cells contribute to myocardial regeneration are still unclear. In the present study, most of the observed benefit might be attributed to enhanced angiogenesis, increased cardiomyocyte turnover, and c-Kit cell proliferation in THI-treated mice, as evidenced by the immunohistological analysis. However, and in agreement with the available published data, we did not observe significant upregulation of cardiac genes in the circulating bone marrow cells or transdifferentiation of mobilized BM cells to functional cardiomyocytes. An increasing body of evidence suggests a limited role for nonhematopoietic BMSPC differentiation into cardiomyocytes after injury and

a more prominent paracrine effect, leading to reduced apoptosis and enhanced angiogenesis [43, 44]. Although we showed similar numbers of GFP⁺ cells in the remote zone, the rate of angiogenesis increased, suggesting the predominance of paracrine effects. It is important to note that although we found enhanced endothelial gene expression in PB cells after MI and increased capillary density, in particular, with THI treatment, we cannot exclude other pathways initiated by myocardial injury to be responsible for increased expression of endothelial genes and angiogenesis in our model. Nonetheless, THI treatment augmented this existing phenomenon and could be a viable therapeutic target in future studies. Additionally, although we did not specifically address the role of S1P-mediated pre- and postconditioning signaling in cardiac function improvement, we think it is unlikely that our observations resulted from these phenomena, because we administered THI on the fourth day after MI, which is beyond the window of benefit observed with pre- or postconditioning. Additionally, we think that the late improvements in cardiac function were unlikely to reflect persistent elevation of S1P by THI, because its levels returned to control levels by 10 days after MI.

Although upregulation of S1P was predicted to occur with SPL inhibition, the increase in C1P was unexpected. C1P is metabolized by lipid phosphate phosphatases (lipid phosphate phosphatases 1–3) [45, 46], and SPL is not thought to degrade

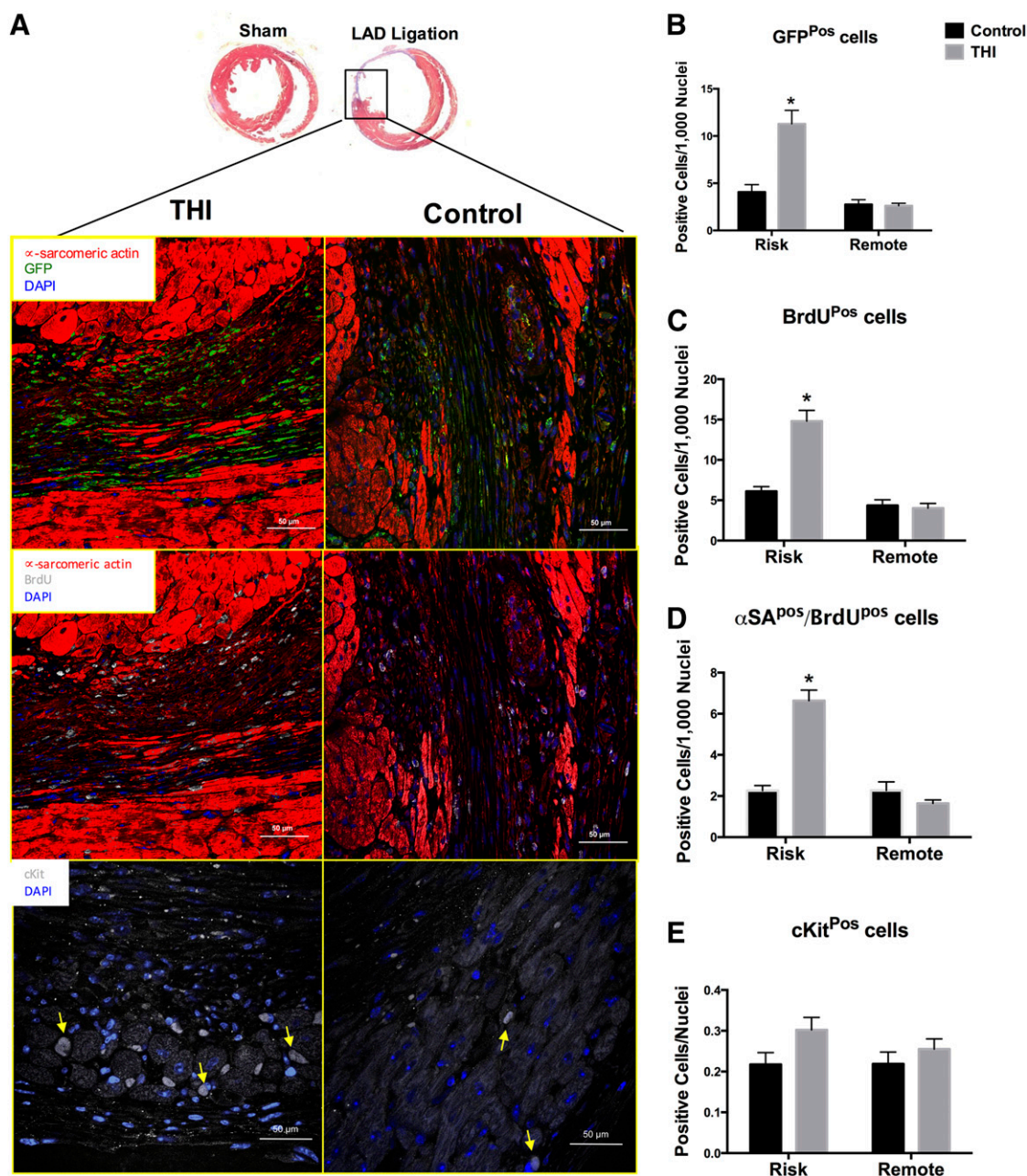


Figure 6. Enhanced bone marrow stem cell homing and cardiomyocyte turnover in THI-treated mice after myocardial infarction ($n = 4$ per group). GFP⁺ bone marrow cells in the infarct border of LV sections after myocardial infarction were quantified after immunofluorescent staining and confocal microscopy. Proliferating cardiomyocytes were labeled with BrdU. **(A):** Representative images of GFP staining in infarct border of THI-treated mice (left) and vehicle-treated mice (right) showing a significantly higher number of GFP⁺ cells in the THI-treated mice (top). BrdU staining of infarct border showing enhanced cell turnover with higher BrdU⁺ cells in THI-treated compared with vehicle-treated mice (middle). Representative images of c-Kit-stained cells (arrows) in the infarct border (risk zone) cross-sections showing higher counts in THI-treated mice (left). **(B):** Quantitative analysis of GFP⁺ cells in the infarct border (risk area) and remote zone showing significantly higher number of GFP⁺ cells in THI-treated mice in the risk area but not in the remote zone. **(C):** Quantitative analysis of BrdU⁺ cells in the infarct border (risk area) and remote zone showing significantly a higher number of BrdU⁺ cells in THI-treated mice in the risk area but not in the remote zone. **(D):** Quantitative analysis of BrdU⁺/ α SA⁺ cells in the infarct border (risk area) and remote zone showing significantly a higher number of BrdU⁺/ α SA⁺ cells in THI-treated mice in the risk area but not in the remote zone. **(E):** Quantitative analysis of c-Kit-positive cells demonstrating their increased numbers in peri-infarct region in THI-supplemented mice after AMI. Values are presented as mean \pm SEM (*, $p < .05$ vs. vehicle control). Abbreviations: α SA, α -sarcomeric actin; BrdU, bromodeoxyuridine; DAPI, 4',6-diamidino-2-phenylindole; GFP, green fluorescent protein; LAD, left anterior descending coronary artery; THI, tetrahydrobutylimidazole.

C1P. However, SPL inhibition results in increases in total sphingosine and ceramide pools, which are the necessary substrates for C1P synthesis [47]. C1P levels are also upregulated in SPLKO mice (unpublished data). Thus, the elevation observed in C1P levels might be an indirect consequence of SPL inhibition. This

is a significant finding, because C1P signaling is both anti-apoptotic and contributes to stem cell mobilization [34, 48]. More detailed studies are necessary to dissect the relative contributions of S1P and C1P to the phenomena we have reported.

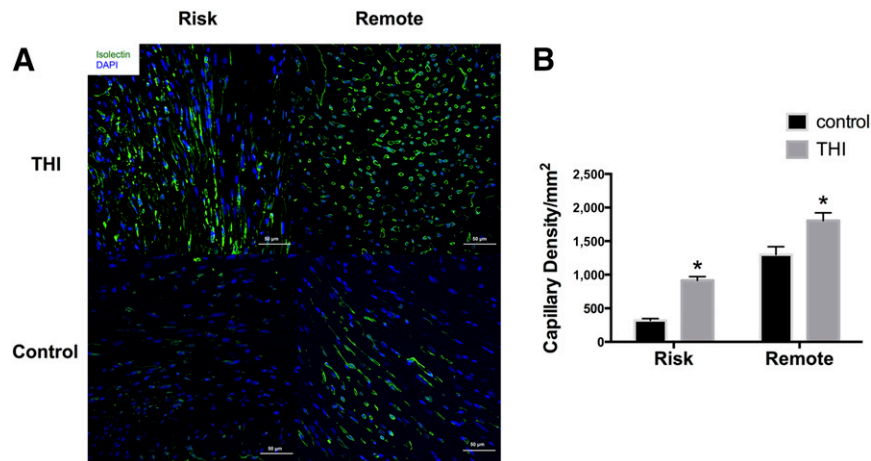


Figure 7. THI supplementation increases capillary density in infarcted mice ($n = 3$ per group). Capillaries in the peri-infarct risk area of the left ventricle were labeled with FITC-conjugated isolectin B4 and counted. **(A):** Representative fluorescent confocal images of FITC-isolectin-stained infarct border (risk zone) and remote area cross-sections from THI-treated and vehicle control-treated mice after myocardial infarction (MI). **(B):** Quantitative analysis of capillary density demonstrating increased peri-infarct region capillary density in THI-supplemented mice after MI. Values are presented as mean \pm SEM (*, $p < .05$ vs. vehicle control). Scale bars = 50 μm . Abbreviations: DAPI, 4',6-diamidino-2-phenylindole; THI, tetrahydroxybutylimidazole.

Most importantly, the present findings have significant translational relevance. Transient posts ischemic SPL inhibition had a positive impact on cardiac function. Specifically, we observed significant improvements in the LV ejection fraction and a reduction in LV diameter and volume at end-systole and end-diastole, suggesting enhanced recovery in functional and remodeling parameters. These findings suggest it is rational to work toward the development and application of therapeutic strategies to ameliorate cardiac dysfunction after ischemic injury. Recently, SPL was characterized as a novel target for the management of clinical conditions [49]. An analog of THI, LX2931, has been characterized as a robust and safe inhibitor of SPL. These findings suggest that SPL inhibition by LX2931 in an AMI model could yield similar therapeutic effects as those presented in our study. We are planning preclinical studies using these agents in myocardial regenerative studies.

CONCLUSION

Our findings have demonstrated that early transient SPL inhibition after MI correlates with increased stem cell mobilization and their homing to the infarct border zones. Augmenting BMSPC mobilization correlated with the formation of new blood vessels and cardiomyocyte and c-Kit cell proliferation. These novel findings at the cellular level were associated with functional cardiac recovery, reduced adverse remodeling, and a decreased scar size. Taken together, these data indicate that pharmacological elevation of bioactive lipid levels can be beneficial in the early phase after cardiac ischemic injury. These findings provide the first evidence

that a carefully timed transient pharmacological upregulation of bioactive lipids after AMI could be therapeutic, because it results in significant cardiac structural and functional improvements.

ACKNOWLEDGMENTS

Dr. Abdel-Latif is supported by the University of Kentucky Clinical and Translational Science Pilot Award (Grant UL1TR000117), the U.K. COBRE Early Career Program (Grant P20 GM103527), and NIH Grant R56 HL124266. Dr. Nagareddy is supported by the NIH Pathway to Independence Award (Grant 1K99HL122505-01). Dr. Ye is supported by the T32 grant (Grant HL091812). Dr. Wysoczynski is supported by the American Heart Association Scientist Development Grant (Grant 13SDG14560005). Dr. Ratajczak is supported by NIH Grants 2R01 DK074720 and R01HL112788.

AUTHOR CONTRIBUTIONS

Y.M.K., S.S.S., M.Z.R., and A.J.M.: conception and design, data analysis and interpretation, manuscript writing; P.R.N., S.Y., and M.W.: collection and/or assembly of data, data analysis and interpretation; A.A., E.G., M.S., J.A.B., R.A., R.P., M.S., and Z.H.P.: collection and/or assembly of data; A.A.-L.: conception and design, data analysis and interpretation, provision of study material or patients, financial support, manuscript writing.

DISCLOSURE OF POTENTIAL CONFLICTS OF INTEREST

The authors indicated no potential conflicts of interest.

REFERENCES

- 1 Roger VL, Go AS, Lloyd-Jones DM et al. Heart disease and stroke statistics—2011 Update: A report from the American Heart Association. *Circulation* 2011;123:e18–e209.
- 2 McMurray JJ, Pfeffer MA. Heart failure. *Lancet* 2005;365:1877–1889.
- 3 Quaini F, Urbanek K, Beltrami AP et al. Chimerism of the transplanted heart. *N Engl J Med* 2002;346:5–15.
- 4 Bergmann O, Bhardwaj RD, Bernard Set al. Evidence for cardiomyocyte renewal in humans. *Science* 2009;324:98–102.
- 5 Hsieh PC, Segers VF, Davis ME et al. Evidence from a genetic fate-mapping study that stem cells refresh adult mammalian cardiomyocytes after injury. *Nat Med* 2007;13:970–974.
- 6 Abdel-Latif A, Zuba-Surma EK, Ziada KM et al. Evidence of mobilization of pluripotent stem cells into peripheral blood of patients with myocardial ischemia. *Exp Hematol* 2010;38:1131.e1–1142.e1.
- 7 Kawada H, Fujita J, Kinjo K et al. Nonhematopoietic mesenchymal stem cells can be mobilized and differentiate into cardiomyocytes after myocardial infarction. *Blood* 2004;104:3581–3587.
- 8 Brehm M, Ebner P, Picard F et al. Enhanced mobilization of CD34(+) progenitor cells expressing cell adhesion molecules in patients with STEMI. *Clin Res Cardiol* 2009;98:477–486.

- 9 Wojakowski W, Tendera M. Mobilization of bone marrow-derived progenitor cells in acute coronary syndromes. *Folia Histochem Cytobiol* 2005;43:229–232.
- 10 Wyderka R, Wojakowski W, Jadczyk T et al. Mobilization of CD34+CXCR4+ stem/progenitor cells and the parameters of left ventricular function and remodeling in 1-year follow-up of patients with acute myocardial infarction. *Mediators Inflamm* 2012;2012:564027.
- 11 Youn SW, Lee SW, Lee J et al. COMP-Ang1 stimulates HIF-1 α -mediated SDF-1 overexpression and recovers ischemic injury through BM-derived progenitor cell recruitment. *Blood* 2011;117:4376–4386.
- 12 Lapidot T, Dar A, Kollet O. How do stem cells find their way home? *Blood* 2005;106:1901–1910.
- 13 Ratajczak MZ, Kim CH, Abdel-Latif A et al. A novel perspective on stem cell homing and mobilization: Review on bioactive lipids as potent chemoattractants and cationic peptides as underappreciated modulators of responsiveness to SDF-1 gradients. *Leukemia* 2012;26:63–72.
- 14 Agarwal U, Ghalayini W, Dong F et al. Role of cardiac myocyte CXCR4 expression in development and left ventricular remodeling after acute myocardial infarction. *Circ Res* 2010;107:667–676.
- 15 Karapetyan AV, Klyachkin YM, Selim S et al. Bioactive lipids and cationic antimicrobial peptides as new potential regulators for trafficking of bone marrow-derived stem cells in patients with acute myocardial infarction. *Stem Cells Dev* 2013;22:1645–1656.
- 16 Ratajczak MZ, Lee H, Wysocki M et al. Novel insight into stem cell mobilization—plasma sphingosine-1-phosphate is a major chemoattractant that directs the egress of hematopoietic stem progenitor cells from the bone marrow and its level in peripheral blood increases during mobilization due to activation of complement cascade/membrane attack complex. *Leukemia* 2010;24:976–985.
- 17 Means CK, Brown JH. Sphingosine-1-phosphate receptor signalling in the heart. *Cardiovasc Res* 2009;82:193–200.
- 18 Vessey DA, Li L, Honbo N et al. Sphingosine 1-phosphate is an important endogenous cardioprotectant released by ischemic pre- and postconditioning. *Am J Physiol Heart Circ Physiol* 2009;297:H1429–H1435.
- 19 Bandhuvula P, Honbo N, Wang GY et al. S1P lyase: A novel therapeutic target for ischemia-reperfusion injury of the heart. *Am J Physiol Heart Circ Physiol* 2011;300:H1753–H1761.
- 20 Gao E, Lei YH, Shang X et al. A novel and efficient model of coronary artery ligation and myocardial infarction in the mouse. *Circ Res* 2010;107:1445–1453.
- 21 Schwab SR, Pereira JP, Matloubian M et al. Lymphocyte sequestration through S1P lyase inhibition and disruption of S1P gradients. *Science* 2005;309:1735–1739.
- 22 Dai S, Yuan F, Mu J et al. Chronic AMD3100 antagonism of SDF-1 α -CXCR4 exacerbates cardiac dysfunction and remodeling after myocardial infarction. *J Mol Cell Cardiol* 2010;49:587–597.
- 23 Mathews TP, Kennedy AJ, Kharel Y et al. Discovery, biological evaluation, and structure-activity relationship of amidine based sphingosine kinase inhibitors. *J Med Chem* 2010;53:2766–2778.
- 24 Selim S, Sunkara M, Salous AK et al. Plasma levels of sphingosine 1-phosphate are strongly correlated with haematocrit, but variably restored by red blood cell transfusions. *Clin Sci (Lond)* 2011;121:565–572.
- 25 Dreyer WJ, Michael LH, Nguyen T et al. Kinetics of C5a release in cardiac lymph of dogs experiencing coronary artery ischemia-reperfusion injury. *Circ Res* 1992;71:1518–1524.
- 26 Sun Y, Weber KT. Infarct scar: A dynamic tissue. *Cardiovasc Res* 2000;46:250–256.
- 27 Abdel-Latif A, Zuba-Surma EK, Ziada KM et al. Evidence of mobilization of pluripotent stem cells into peripheral blood of patients with myocardial ischemia. *Exp Hematol* 2010;38:1131.e1–1142.e1.
- 28 Zuba-Surma EK, Kucia M, Dawn B et al. Bone marrow-derived pluripotent very small embryonic-like stem cells (VSELs) are mobilized after acute myocardial infarction. *J Mol Cell Cardiol* 2008;44:865–873.
- 29 Poitevin S, Cussac D, Leroyer AS et al. Sphingosine kinase 1 expressed by endothelial colony-forming cells has a critical role in their revascularization activity. *Cardiovasc Res* 2014;103:121–130.
- 30 Klyachkin YM, Karapetyan AV, Ratajczak MZ et al. The role of bioactive lipids in stem cell mobilization and homing: Novel therapeutics for myocardial ischemia. *Biomed Res Int* 2014;2014:653543.
- 31 van den Borne SW, Diez J, Blankesteijn WM et al. Myocardial remodeling after infarction: The role of myofibroblasts. *Nat Rev Cardiol* 2010;7:30–37.
- 32 Mierzejewska K, Klyachkin YM, Ratajczak J et al. Sphingosine-1-phosphate-mediated mobilization of hematopoietic stem/progenitor cells during intravascular hemolysis requires attenuation of SDF-1-CXCR4 retention signaling in bone marrow. *Biomed Res Int* 2013;2013:814549.
- 33 Ratajczak MZ, Suszynska M, Borkowska S et al. The role of sphingosine-1 phosphate and ceramide-1 phosphate in trafficking of normal stem cells and cancer cells. *Expert Opin Ther Targets* 2014;18:95–107.
- 34 Kim C, Schneider G, Abdel-Latif A et al. Ceramide-1-phosphate regulates migration of multipotent stromal cells and endothelial progenitor cells—Implications for tissue regeneration. *STEM CELLS* 2013;31:500–510.
- 35 Ratajczak MZ, Borkowska S, Ratajczak J. An emerging link in stem cell mobilization between activation of the complement cascade and the chemotactic gradient of sphingosine-1-phosphate. *Prostaglandins Other Lipid Mediat* 2013;104-105:122–129.
- 36 Wojakowski W, Tendera M, Kucia M et al. Mobilization of bone marrow-derived Oct-4+ SSEA-4+ very small embryonic-like stem cells in patients with acute myocardial infarction. *J Am Coll Cardiol* 2009;53:1–9.
- 37 Golan K, Vagima Y, Ludin A et al. S1P promotes murine progenitor cell egress and mobilization via S1P1-mediated ROS signaling and SDF-1 release. *Blood* 2012;119:2478–2488.
- 38 Orlic D, Kajstura J, Chimenti S et al. Mobilized bone marrow cells repair the infarcted heart, improving function and survival. *Proc Natl Acad Sci USA* 2001;98:10344–10349.
- 39 Abdel-Latif A, Bolli R, Zuba-Surma EK et al. Granulocyte colony-stimulating factor therapy for cardiac repair after acute myocardial infarction: A systematic review and meta-analysis of randomized controlled trials. *Am Heart J* 2008;156:216–226.
- 40 Iwanaga K, Takano H, Ohtsuka M et al. Effects of G-CSF on cardiac remodeling after acute myocardial infarction in swine. *Biochem Biophys Res Commun* 2004;325:1353–1359.
- 41 Moazzami K, Roohi A, Moazzami B. Granulocyte colony stimulating factor therapy for acute myocardial infarction. *Cochrane Database Syst Rev* 2013;5:CD008844.
- 42 Jeevanantham V, Butler M, Saad A et al. Adult bone marrow cell therapy improves survival and induces long-term improvement in cardiac parameters: A systematic review and meta-analysis. *Circulation* 2012;126:551–568.
- 43 Zuba-Surma EK, Guo Y, Taher H et al. Transplantation of expanded bone marrow-derived very small embryonic-like stem cells (VSEL-SCs) improves left ventricular function and remodeling after myocardial infarction. *J Cell Mol Med* 2011;15:1319–1328.
- 44 Loffredo FS, Steinhauser ML, Gannon J et al. Bone marrow-derived cell therapy stimulates endogenous cardiomyocyte progenitors and promotes cardiac repair. *Cell Stem Cell* 2011;8:389–398.
- 45 Sciorra VA, Morris AJ. Roles for lipid phosphate phosphatases in regulation of cellular signaling. *Biochim Biophys Acta* 2002;1582:45–51.
- 46 Brindley DN, English D, Pilquill C et al. Lipid phosphate phosphatases regulate signal transduction through glycerolipids and sphingolipids. *Biochim Biophys Acta* 2002;1582:33–44.
- 47 Reiss U, Oskouian B, Zhou J et al. Sphingosine-phosphate lyase enhances stress-induced ceramide generation and apoptosis. *J Biol Chem* 2004;279:1281–1290.
- 48 Gómez-Muñoz A, Kong JY, Salh B et al. Ceramide-1-phosphate blocks apoptosis through inhibition of acid sphingomyelinase in macrophages. *J Lipid Res* 2004;45:99–105.
- 49 Bagdanoff JT, Donoviel MS, Nouraldeen A et al. Inhibition of sphingosine 1-phosphate lyase for the treatment of rheumatoid arthritis: Discovery of (E)-1-(4-((1R,2S,3R)-1,2,3,4-tetrahydroxybutyl)-1H-imidazol-2-yl)ethanone oxime (LX2931) and (1R,2S,3R)-1-(2-(isoxazol-3-yl)-1H-imidazol-4-yl)butane-1,2,3,4-tetraol (LX2932). *J Med Chem* 2010;53:8650–8662.



See www.StemCellsTM.com for supporting information available online.